

# The role of meteoric influx and the geomagnetic disturbance on the seasonal forming of sporadic E over Europe

Wolfgang Kaufmann<sup>1</sup>

The seasonal forming of a sporadic E (Es) layer over Europe was analysed by Es layer critical frequency data from six European ionosondes, the planetary Ap-Index and radio meteor echo counts from three European stations. The influence of seasonal varying meteoric influx and geomagnetic disturbance of Earth's magnetic field on the seasonal forming of the Es layer was found to be ambivalent. The occurrence of a high electron density Es layer coincided remarkably with the level of the combined number of counted meteors and geomagnetic Ap Index from February to September whereas this was not true for the remaining months.

Received 2022 March 2

## 1 Introduction

A sporadic E (Es) layer is a thin highly ionised temporary layer in the atmosphere at about 100 km height. According to the widely accepted Windshear Theory (Whitehead, 1961; Axford, 1963; Whitehead, 1997) the central forces of the forming process of a sporadic E layer are the Earth's magnetic field, the atmospheric metallic ion concentration and wind shears in horizontal neutral winds in the mesosphere/lower thermosphere, MLT (for a comprehensive review see Haldoupis, 2011). The evolving of a thin layer of compressed positively charged metallic ions between two stacked reverse wind flows by geomagnetic Lorentz forcing is followed by the attraction of free electrons moving along the magnetic field lines to neutralize this charge. The resulting clouds

with a high density of free electrons represent the Es layer and are responsible for the refraction of radio waves. Solar driven oscillations of the wind flows in the MLT modulate the diurnal forming of Es in a characteristic manner that can be observed even by means of an amateur (Kaufmann, 2021). Furthermore, the mid-latitude forming of Es shows a perspicuous seasonal dependence that is marked by a pronounced summer maximum.

Haldoupis et al. (2007) suggested that the seasonal sporadic E layer forming is determined by the supply of the atmosphere with metallic ions originating from incoming ablating meteoroids. However, e.g. Mubasshir Shaikh et al. (2021) denied such correlation over the Arabian peninsula. No clear picture can be gained from literature about the influence of the meteoric influx on Es forming. Hence, the aim of this study is to analyse the situation in Europe. Forward scattered radio waves off ionised meteor trails were employed as an estimate of the influx of meteors over Europe. These data were

<sup>1</sup>Lindenweg 1e, 31191 Algermissen, Germany. Email: [contact@ars-electromagnetica.de](mailto:contact@ars-electromagnetica.de)

IMO bibcode WGN-502-kaufmann-sporadic  
NASA-ADS bibcode 2022JIMO...50...62K

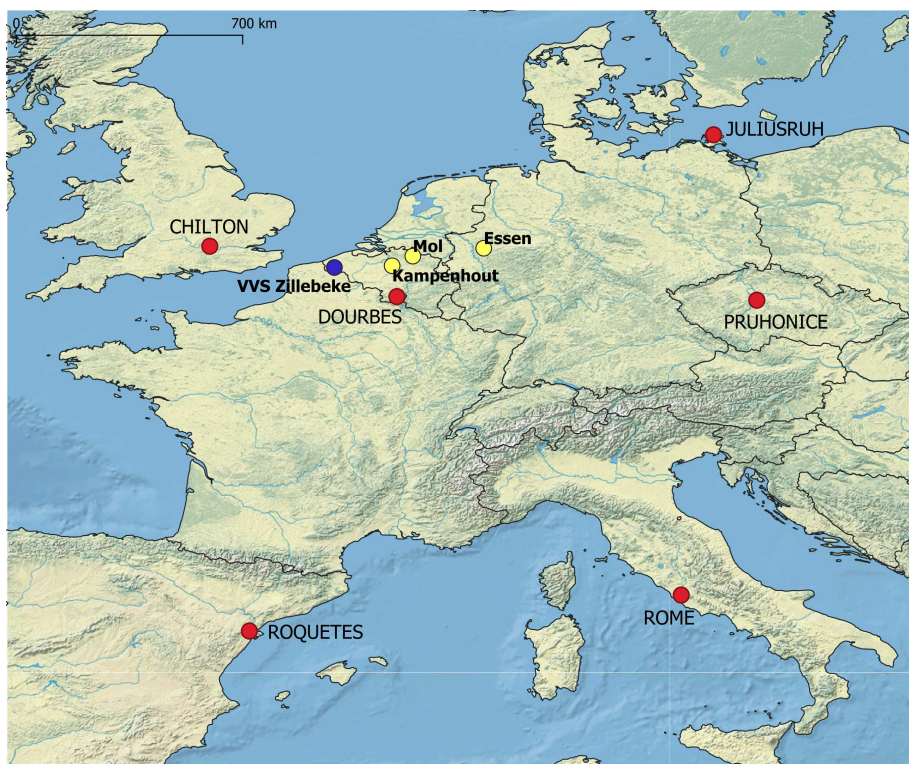


Figure 1 – Positions of the six Ionosondes (red), the three radio observation stations (yellow) and the applied transmitter (blue). Map made with Natural Earth.

taken from three receiving radio stations using the same continuously transmitting radio frequency beacon. This gives most homogenous data-sets.

The occurrence of Es was derived from daily Es layer critical frequency ( $f_o E_s$ ) of 6 different European ionosondes. Thereby, the level of the frequency directly depends on the concentration of free electrons in the Es layer. A one year time series of the  $f_o E_s$  was considered together with the corresponding daily count rates of radio meteors. Additionally the daily geomagnetic Ap-Index was included in the analysis as a suspected influencing factor of Es-forming.

## 2 Data and Methods

The analysis was performed for the time period 2020-01-01 to 2020-12-31. The radio observed number of daily meteors were provided by F. Verbelen, Kampenhout, C. Steyaert, Mol and WHS, Essen. They employed the VVS-beacon at Zillebeke as transmitter at 49.99 MHz. From the European ionosondes Chilton, Juliusruh, Pruhonice, Dourbes, Roquetes and Rome data about Es layer critical frequency ( $f_o E_s$ ) were retrieved from the Lowell GIRO Data Center (LGDC)<sup>a</sup>. The ionosondes were picked approximately on a circle around these meteor measuring stations or being directly adjacent, respectively, see Figure 1. The planetary Ap-Indices were downloaded from the GFZ German Research Centre for Geosciences<sup>b</sup> (Matzka et al., 2021a).

Each ionosonde performed a couple of  $f_o E_s$  measurements per day. For reducing them to a one day value the  $f_o E_s$  maximum value per day and ionosonde was taken. The maximum value was chosen to focus on the highest electron densities evolving on each day. Thereby only those measurements were taken into account that had an auto-scaling confidence score  $\geq 75$ . The confidence score is a measure of the reliability of Es detection by the ionosonde's feature recognition algorithm. From the 8 daily 3h-Ap-Index measurements the maximum-value per day was taken. From the three radio meteor observing stations daily count rates (dCR) were derived. To each of these time series a 25-day moving average was applied. Hereby, short-term daily fluctuations were balanced out, long-term trends became visible. Subsequently the smoothed time series were normalised to 0–1. From the time series of the six ionosondes as well as of the three radio meteor observing stations a daily mean was calculated. Thus three basic measures were available:  $f_o E_s$  (trend),  $Ap_{25}$  (trend) and  $dCR_{25}$  (trend). For further smoothing at least these three time series were decomposed into seasonal, trend, and residual components by a statistical time series algorithm. From this the trend component was used whereby calculating a 10 day trend was found to be appropriate:  $f_o E_s$  (trend),  $Ap_{25}$  (trend) and  $dCR_{25}$  (trend).

## 3 Results

Figure 2 shows the course of  $f_o E_s$  (trend),  $Ap_{25}$  (trend) and  $dCR_{25}$  (trend). Looking at the  $f_o E_s$  (trend) curve it should be pointed out, that an Es layer obviously was present throughout the year. However, its electron density only shows a pronounced summer maximum in May to August, a small local maximum in October and a second small local maximum in January. The  $dCR_{25}$  (trend) curve shows two broad maxima: one in May to August and one in October to December. Also the  $Ap_{25}$  (trend) has a seasonal shaped time course which can be observed generally: Matzka et al. (2021b) found a marked seasonal variation with equinoctial maxima analysing the period 1932–2019.

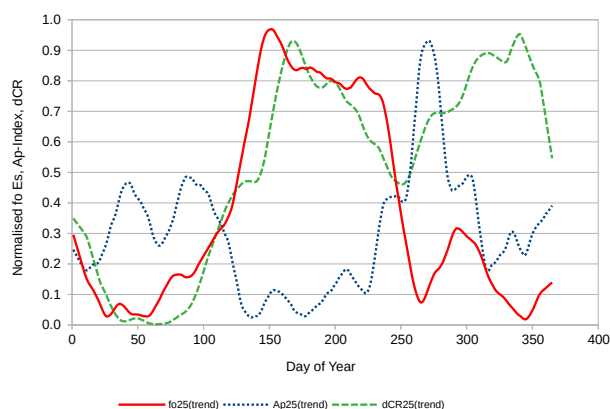


Figure 2 – The smoothed and normalised curve progression of critical frequency of the Es layer ( $f_o E_s$  (trend), red solid line), the meteor counts ( $dCR_{25}$  (trend), dashed green line) and planetary A-Index ( $Ap_{25}$  (trend), blue dotted line) in the year 2020.

The occurrence of the summer maxima of both the  $f_o E_s$  (trend) and  $dCR_{25}$  (trend) is astonishingly synchronous. The same is true for the minimum of  $Ap_{25}$  (trend). Combining  $dCR_{25}$  and  $Ap_{25}$  could lead to an even better approximation to  $f_o E_s$ . Therefore, a simple additive model was adopted:

$$f(\text{Ap}, \text{dCR}) = -\text{Ap}_{25}(\text{trend}) + \text{dCR}_{25}(\text{trend})$$

The result is depicted in Figure 3. In the time period from about February–September the  $f(\text{Ap}, \text{dCR})$  curve correlates well with the  $f_o E_s$  (trend) curve. The small

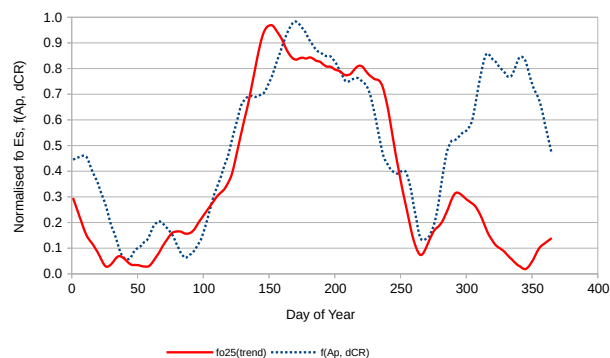


Figure 3 – The smoothed and normalised curve progression of critical frequency of the Es layer ( $f_o E_s$  (trend), red solid line) and combined meteor counts / Ap-Indices ( $f(\text{Ap}, \text{dCR})$ , blue dotted line) in the year 2020.

<sup>a</sup><http://space.info/SMWG/Observatory/GIRO>

<sup>b</sup><https://www.gfz-potsdam.de/kp-index/>

local October maximum of  $f_{o_{25}}$  Es (trend) initially follows the  $f(\text{Ap}, \text{dCR})$  curve. However, with increasing temporal distance from the summer the degree of correlation decreases fast. Especially in November and December both curves show the largest deviation between them.

## 4 Discussion

Six European ionosondes being arranged around the transmitter/receiver set provided a geographical and statistical solid base for the analysis. The normalisation of all data time series eliminated individual differences in the values of the measured data and emphasised their trends. Choosing three radio stations listening to same transmitter guaranteed a radio meteor detection area lying in between the location of the six ionosondes. Briefly, the area where radio meteors can be detected is defined by ellipsoids with the position of the receiver and the transmitter as foci and the trajectories of the meteors tangential to these ellipsoids (Rendtel & Arlt, 2015). Employing three stations not only reduced the influence of possible false positives but also enhanced the meteor detection area. Furthermore the influence of the individual transmitter – meteor-trajectory – receiver geometries on the local meteor detection-rates was relativized.

As shown in Figure 3 the additive combination of  $\text{dCR}_{25}$  and  $\text{Ap}_{25}$  was able to reproduce the course of  $f_{o_{25}}$  Es remarkably well from February to September. To evaluate their match in more detail the difference between the time series of  $f_{o_{25}}$  Es (trend) and  $f(\text{Ap}, \text{dCR})$  was calculated per each day and plotted in Figure 4. The standard deviation (sd) of the calculated difference was used as a matching-criterion. The range of one sd was centred around the zero line in Figure 4. Thus the time periods could be estimated in which the difference between  $f_{o_{25}}$  Es (trend) and  $f(\text{Ap}, \text{dCR})$  is within the span of one sd. Using this approach an essentially continuous match was found from February to September 2020 (days 32–273, corresponding to February 1<sup>st</sup> and September 29<sup>th</sup>, respectively).

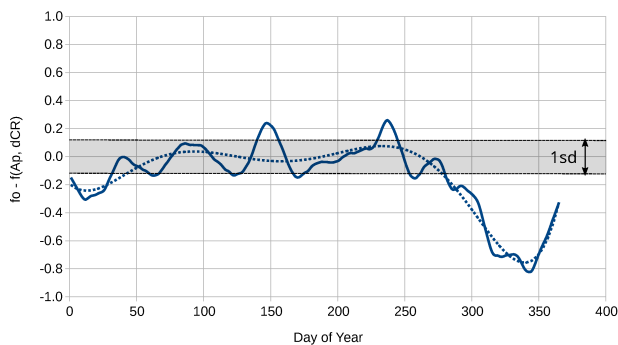


Figure 4 – Plot of the difference between  $f_{o_{25}}$  Es and  $f(\text{Ap}, \text{dCR})$  as shown in Figure 3. The standard deviation centred around zero and a smoothing polynomial of 6<sup>th</sup> order (dotted line) are indicated.

This result does not support any of the conflicting data in the literature. On the one hand there is a remarkable match in the temporal evolution of the combined meteor count rates / Ap-Indices and the Es layer critical frequency from February to September. On the other hand the same factor combination is not able to explain the low electron density of the Es layer from October to January. Following, it may suggest that the seasonal variation of these two factors do not seem to play a key role in the seasonal variation of Es forming generally or at least during autumn-/winter. However, their surprising correlation with the Es occurrence during nine months of the year may assign them a modulating effect.

An explanation for the diverse findings could result from different methods used to estimate the meteoric influx. None of the used techniques (radar backscatter, forward scatter, visual) is capable to deliver a continuous 24 h observation based on a spatially uniform responsiveness over the whole hemisphere. The distribution of detectable meteoroid masses also differs between the techniques and observing stations. This may strongly bias the estimate of meteoric influx.

Moreover, it should be kept in mind, that seasonal different wind regimes in the MLT could be responsible for the seasonal variation of Es layer forming. Recently, a large number of neutral wind measurements from the Ionospheric Connection Explorer (ICON) mission (Immel et al., 2018) became available, providing an opportunity for direct comparison of Es with the local wind shear.

## 5 Conclusion

No unequivocal information about the role of the seasonal varying meteoric influx and planetary A-Index could be gained to explain the seasonal variation of Es layer forming over Europe. The assumption that the seasonal variation of these two factors are the main drivers of the seasonal occurrence of Es could not be supported by this study. On the other hand, the influence of these two factors cannot be denied. At least their seasonal variation may have a modulating effect.

## Acknowledgment

Meteor data kindly were provided by Felix Verbeelen (personal communication) as well as Chris Steyaert and WHS Essen via RMOB<sup>c</sup>. This paper uses data from the Juliusruh Ionosonde which is owned by the Leibniz Institute of Atmospheric Physics Kuehlungsborn, from the ionospheric observatory in Dourbes, owned and operated by the Royal Meteorological Institute (RMI) of Belgium, from the Observatory of Ebre, Spain, from the Chilton ionosonde operated by the Rutherford Appleton Laboratory, from the Průhonice Observatory of the Institute of Atmospheric Physics CAS and from the Rome Observatory of the Istituto Nazionale di Geofisica e Vulcanologia. The Ap-Index is taken from the GFZ German Research Centre for Geosciences.

<sup>c</sup><https://www.rmob.org/index.php>

## References

- Axford W. I. (1963). “The Formation and Vertical Movement of Dense Ionized Layers in the Ionosphere Due to Neutral Wind Shears”. *Journal of Geophysical Research*, **68:3**, 769–779.
- Haldoupis C. (2011). “A tutorial review on sporadic e layers”. In Abdu M. A. and Pancheva D., editors, *Aeronomy of the Earth’s Atmosphere and Ionosphere*, pages 381–394. Springer Science+Business Media B.V.
- Haldoupis C., Pancheva D., Singer W., Meek C., and MacDougall J. (2007). “An explanation for the seasonal dependence of midlatitude sporadic E layers”. *Journal of Geophysical Research (Space Physics)*, **112:A6**, A06315.
- Immel T. J., England S. L., Mende S. B., Heelis R. A., Englert C. R., Edelstein J., Frey H. U., Korpela E. J., Taylor E. R., Craig W. W., Harris S. E., Bester M., Bust G. S., Crowley G., Forbes J. M., Gérard J. C., Harlander J. M., Huba J. D., Hubert B., Kamalabadi F., Makela J. J., Maute A. I., Meier R. R., Raftery C., Rochus P., Siegmund O. H. W., Stephan A. W., Swenson G. R., Frey S., Hysell D. L., Saito A., Rider K. A., and Sirk M. M. (2018). “The Ionospheric Connection Explorer Mission: Mission Goals and Design”. *Space Science Reviews*, **214:1**, 1–36.
- Kaufmann W. (2021). “Study of Sporadic E Occurrence in Europe 2021”. *WGN, Journal of the IMO*, **49:5**, 114–119.
- Matzka J., Bronkalla O., Tornow K., Elger K., and Stolle C. (2021b). “Geomagnetic Kp index. V. 1.0.”. <https://doi.org/10.5880/Kp.0001>.
- Matzka J., Stolle C., Yamazaki Y., Bronkalla O., and Morschhauser A. (2021a). “The Geomagnetic Kp Index and Derived Indices of Geomagnetic Activity”. *Space Weather*, **19:5**, e02641.
- Mubasshir Shaikh M., Gopakumar G., Abdulla Al-owais A., Essa Sharif M., and Fernini I. (2021). “Contribution of meteor flux in the occurrence of sporadic-E (Es) layers over the Arabian Peninsula”. *Annales Geophysicae*, **39:3**, 471–478.
- Rendtel J. and Arlt R. (2015). *Handbook for Meteor Observers*. International Meteor Organization, Potsdam.
- Whitehead D. (1997). “Sporadic E — A Mystery Solved? Part 2”. *QST*, pages 38–42.
- Whitehead J. D. (1961). “The formation of the sporadic-E layer in the temperate zones”. *Journal of Atmospheric and Terrestrial Physics*, **20:1**, 49–58.

---

Handling Editor: Javor Kac